In: Port and Ocean Engineering in the Arctic Conference (POAC'01) Proceedings, Vol. 3, Ottawa, Canada. pp. 1405-1412, 2001.

HEAT BUDGET AND DECAY OF CLEAN AND SEDIMENT-LADEN SEA ICE OFF THE NORTHERN COAST OF ALASKA

Karoline Frey[1], Hajo Eicken[1], Don K. Perovich[2], Tom C. Grenfell[3], Bonnie Light[3], Lewis H. Shapiro[1], Aaron P. Stierle[1]

[1]Geophysical Institute, University of Alaska Fairbanks, Fairbanks, AK 99775-7320, USA
[2]Cold Regions Research and Engineering Laboratory, Hanover, NH 03755-1290
[3]Department of Atmospheric Sciences, University of Washington, Seattle, WA 98195-1640

ABSTRACT

The heat budget and decay of sea ice is strongly affected by the albedo of the surface in the melting season. Sea ice with a high sediment load, as often observed in Arctic coastal regions, has a much lower albedo than clean ice and snow, absorbing a higher fraction of incoming solar radiation. Here, we report measurements of warming and ablation of clean and sediment-laden ice near Barrow, Alaska. After melting of the snow cover, albedos of 0.41 and 0.29 were observed on clean and dirty sea ice. Higher extinction coefficients of sediment-laden sea ice result in absorption of 74 % of the incoming solar radiation within the uppermost 20 cm of the ice. Temperature records show that seasonal warming of the sediment-laden ice is delayed significantly by absorption of radiation in the uppermost layers. However, our observations also indicate that despite greater snow depths over sediment-laden ice, surface ablation rates were higher for dirty than for clean ice.

INTRODUCTION

Sea ice in Arctic coastal regions is often characterized by significant sediment loads that are entrained into the ice during frazil ice formation or through anchor ice rafting over shallow coastal shelves (Osterkamp and Gosink, 1984, Pfirman et al., 1990, Reimnitz et al., 1994, Eicken et al., 2000). Sediments in the top layers of sea ice alter the energy balance by reducing the albedo and hence increasing the amount of absorbed shortwave radiation. This process is expected to have an influence on the energy and mass balance of the ice, especially during the melting season when shortwave irradiative fluxes are highest and the snow on the ice has melted away, uncovering the bare sea ice. In contrast, higher extinction coefficients of sediment-laden ice are expected to significantly reduce the amount of internal solar heating. It is presently not clear, how these contrasting effects combine in either enhancing or reducing the amount of ice melt and timing of ice decay in Arctic coastal areas.

In this study, we will compare the heat budget and decay of clean and highly sediment-laden sea ice off the coast of Barrow, Alaska (for detailed map see Figure 1). Two sites will be considered in detail: clean coastal fast ice in the Chukchi Sea (CS) as well as sediment-laden ice from Elson Lagoon (EL), with a sediment concentration of a few hundreds of mg/l in the upper 0.2-0.4 m.

DATA

Ice thickness and snow depth data as well as temperature profiles have been collected in the ice at the two sites (Figure 1). The temperature measurements were carried out with thermistors (Omega #44031), wired into a Campbell CR10 data logger (precision better than 0.06 K). An important aspect of the experimental set-up is the mounting of the thermistors. The thermistor arrays (5-10 cm spacing) consisted of a separate wire duct, embedded in a polycarbonate-polyethylene matrix of thermal conductivity somewhat lower than that of ice, with the actual thermistors (embedded in a small glass bead) mounted approximately 5 cm away from the duct on a thin support in direct contact with the ice matrix. Ice temperatures down to a depth of 60 cm are shown in Figure 2 from June 1 until the end of the recordings on June 16 from both sites. Thickness and snow cover of the ice were roughly comparable (CS: 1.54 m max. ice thickness, 0.37 m max. snow depth, EL: 1.49 m max. ice thickness, 0.48 m max. snow depth). However, snow depth varied strongly in space both at CS and EL, especially after the melt started.

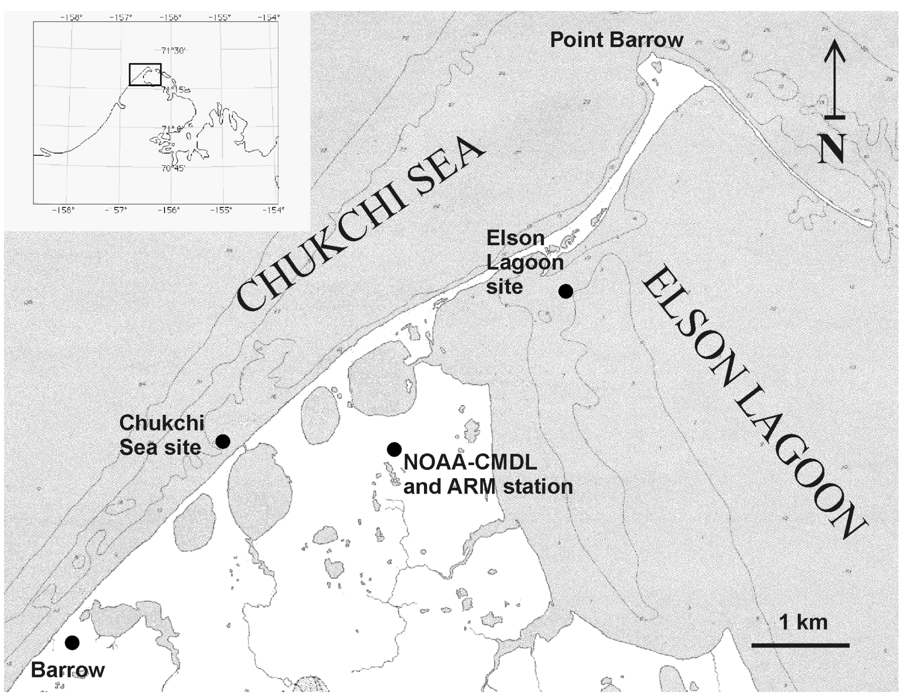

Figure 1: Locations of observations on first-year sea ice near Barrow, Alaska. The solar radiation data were measured at the site of the Atmospheric Radiation Measurement (ARM) Program site.

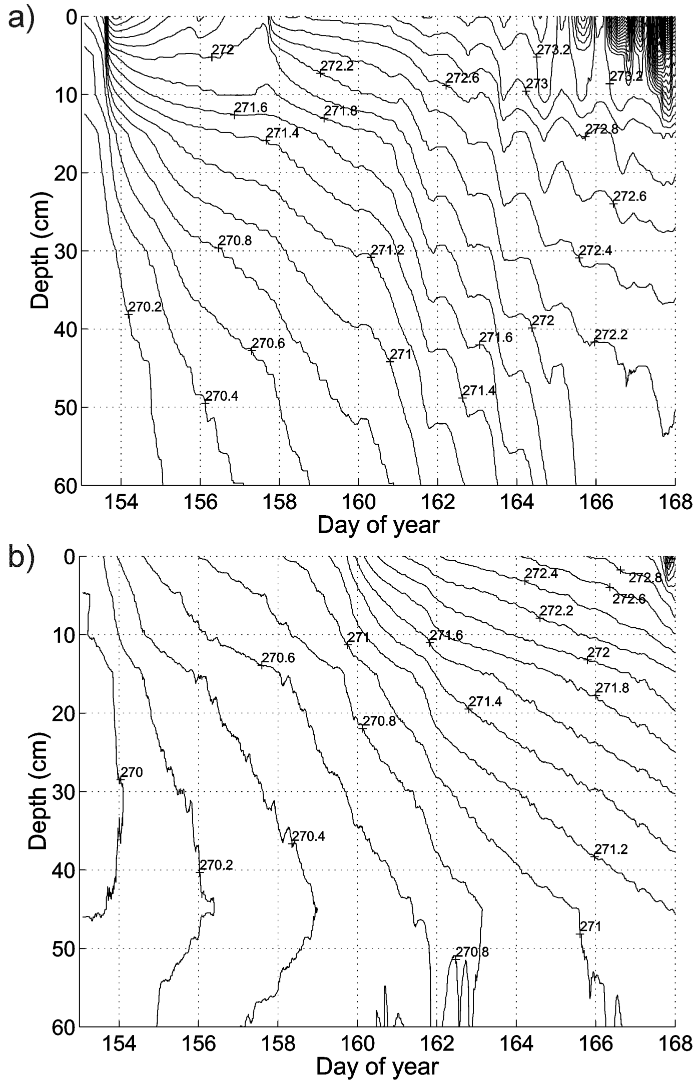

Figure 2: Temperature distribution in the ice from June 1 (day 153 of 2000) to June 16 (day 168 of 2000) in the Chukchi Sea (a) and Elson Lagoon (b).

The daily mean air temperatures measured at the National Atmospheric and Oceanic Administration Climate Monitoring and Diagnostics Laboratory (NOAA-CMDL) meteorological station in Barrow are above freezing for the first time on June 1. However, the onset of melt started earlier, approximately on May 25, at both sites due to the high solar radiation (the sun is above the horizon for 24 h from May 10 on). After this date, the snow cover melted away in appr. 2-3 weeks. Solar radiation was measured at the meteorological station of the Atmospheric Radiation Measurement Program (ARM).

Measurements of the spectrally integrated albedo were carried out frequently along a 200 m profile close to the sites during the melt season with a Kipp & Zonen albedometer, along with readings of snow depth. Figure 3 shows the albedo (averaged along the 200 m line) from the onset of melt to the end of June. Earlier in the season samples had been taken from the sea ice in EL to determine sediment concentration in the ice. The highest sediment loads of 1570 mg/l have been found between 15 and 25 cm depth in the ice (Figure 4), the uppermost layer contains 400 mg/l (dark brown ice) and below 35 cm the sediment concentration decreases to 60 mg/l (moderately discolored ice) and lower. In previous years, sediment concentration in the clean CS ice of some 10 mg/l (slight to no visible discoloration) have been found in the top layers, below, the concentration is even lower.

RESULTS AND DISCUSSION

We found significant sediment concentrations in the sea ice in Elson Lagoon in the winter of '99/00 (Figure 4). The high sediment load does not influence the heat and mass balance of the ice during the winter, but it has a significant impact in the melting season after the snow has melted approximately on June 13-16. The bare surface of sediment-laden ice had a significantly lower albedo, α=0.29, than the snow, α>0.9, and the clean ice, α=0.41, found in the Chukchi Sea. This allows a greater portion of the incoming solar radiation to penetrate the ice and heat it internally. The extinction coefficient determines how much of the shortwave radiation is transmitted to lower layers in the ice. Beer's law,

$$I(z,\lambda) = I_0(\lambda) e^{-\kappa(\lambda) z}, \quad (1)$$

describes attenuation of solar radiation I_0 at the surface of wavelength λ at depth z in the ice, where $I(z,\lambda)$ is the absorbed portion of the incoming radiation and $\kappa(\lambda)$ the extinction coefficient that accounts for attenuation through both absorption and scattering of light by inclusions in the ice (Perovich, 1998). Extinction of solar radiation as well as the albedo, and consequently internal heating through radiation, depends strongly on the sediment load of the ice (Light et al., 1998). The portion of the incoming solar radiation $F\downarrow_{sw}$ that is transmitted to the ice and possibly the ocean underneath,

$$I_0 = (1-\alpha) F\downarrow_{sw}, \quad (2)$$

depends on the albedo α. For the following calculations of light absorption in sea ice we will only use spectrally intergrated values of shortwave radiation, extinction coefficient and albedo.

The daily mean air temperatures measured at the National Atmospheric and Oceanic Administration Climate Monitoring and Diagnostics Laboratory (NOAA-CMDL) meteorological station in Barrow are above freezing for the first time on June 1. However, the onset of melt started earlier, approximately on May 25, at both sites due to the high solar radiation (the sun is above the horizon for 24 h from May 10 on). After this date, the snow cover melted away in appr. 2-3 weeks. Solar radiation was measured at the meteorological station of the Atmospheric Radiation Measurement Program (ARM).

Measurements of the spectrally integrated albedo were carried out frequently along a 200 m profile close to the sites during the melt season with a Kipp & Zonen albedometer, along with readings of snow depth. Figure 3 shows the albedo (averaged along the 200 m line) from the onset of melt to the end of June. Earlier in the season samples had been taken from the sea ice in EL to determine sediment concentration in the ice. The highest sediment loads of 1570 mg/l have been found between 15 and 25 cm depth in the ice (Figure 4), the uppermost layer contains 400 mg/l (dark brown ice) and below 35 cm the sediment concentration decreases to 60 mg/l (moderately discolored ice) and lower. In previous years, sediment concentration in the clean CS ice of some 10 mg/l (slight to no visible discoloration) have been found in the top layers, below, the concentration is even lower.

From June 9 (day 161) on, strong diurnal variations in temperature are apparent at all depths in the CS ice caused by shortwave radiation penetrating into the ice cover (Figure 2 a). Attenuation of the radiation is weak in the clean ice, the amplitude of the variations does not decrease drastically in the upper 60 cm and the maximum occurs approximately at the same time of day, suggesting that the temperature changes are solely caused by solar heating and not heat conduction. In contrast, the EL ice is not affected much by diurnal changes in solar radiation (Figure 2 b). Weak diurnal temperature variation can be observed after June 13 (day 165) down to a depth of 10 cm. The later onset of internal heating by solar radiation is a result of the thicker snow cover on EL that melted away approximately 2-3 days later than on CS. The albedo measurements (Figure 3) reflect the timing of snow melt and formation of melt ponds at both locations. The albedo along the 200 m observation line is drastically reduced between June 5 and June 11 on CS and between June 8 and June 13 on EL indicating the appearance of bare ice and meltponds that have a significantly lower albedo on EL due to high sediment loads. The reduction in albedo is accompanied by an increase in standard deviation along the observation line resulting from spatially variable melt rates that leave patches of snow covered ice next to bare ice and melt ponds. The increase in albedo on CS after June 11 is a result of draining meltponds. From June 13 on, the albedo on EL is lower than on CS, resulting in greater internal heating of the EL ice.

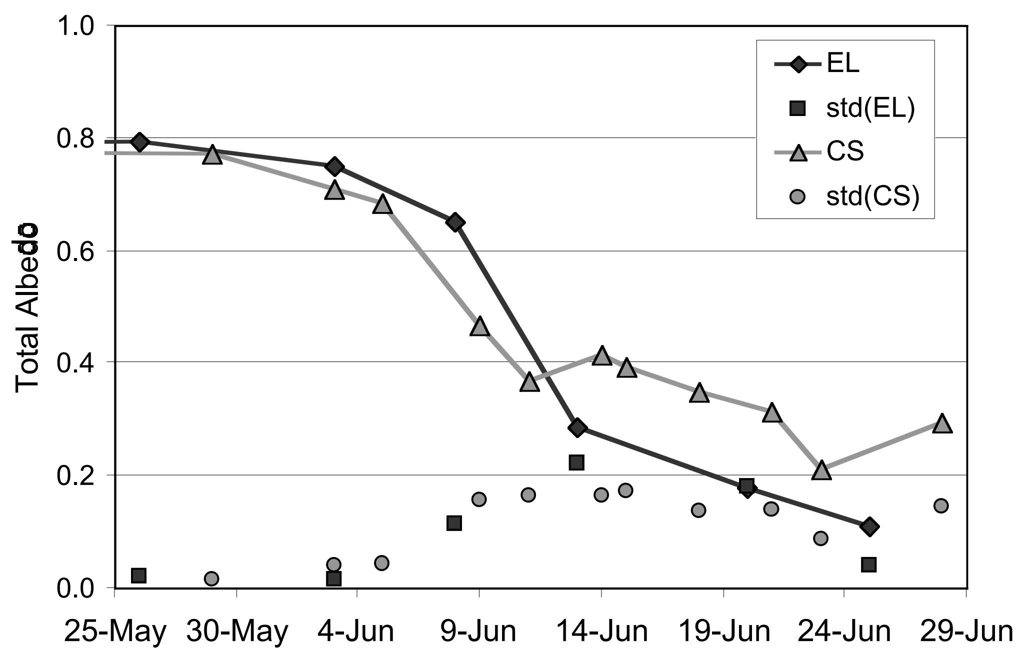

Figure 3: Spectrally integrated albedo averaged over a 200 m observation line on Chukchi Sea and Elson Lagoon during the melting season and standard deviation over each transect.

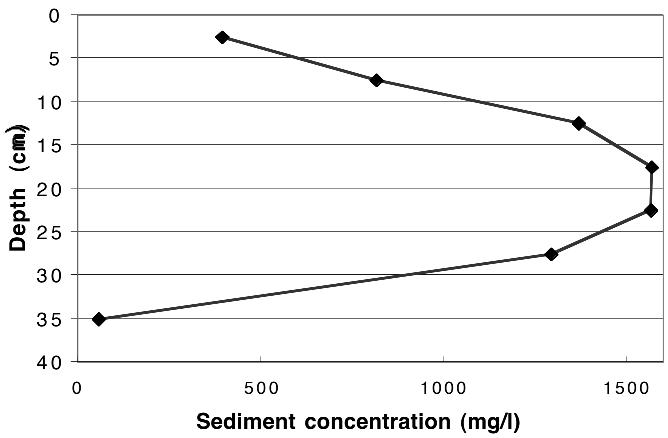

Figure 4: Sediment concentration in the sea ice in Elson Lagoon. The ice below 35 cm did not contain significant loads of sediment, a value of 5 mg/l is assumed.

To compare the amount of solar radiation that is available to heat clean and sediment-laden sea ice on June 14 equation (1) has been solved with extinction coefficients calculated by a radiative transfer model (Light et al., 1998) corresponding to the sediment concentration found in EL (Figure 4) and to very low sediment concentrations (i.e., 10 mg/l in the upper 10 cm and 5 mg/l below) in the case of CS. The amount of shortwave radiation that is transmitted to a certain depth in the ice is shown in Figure 5. Although the surface of the sediment-laden ice receives more radiation, less light is transmitted to the ice at a depth of 5 cm. The amount of light that reaches the dirty ice at a depth of 20 cm is only 2 % of the radiation at the surface, at 30 cm it is negligible, whereas the clean ice at the same depth still receives, respectively, some 35 % and 23 % of the radiation at the surface. This results in greater extent and depth of puddles on the sediment-laden ice. Although it is not clear how

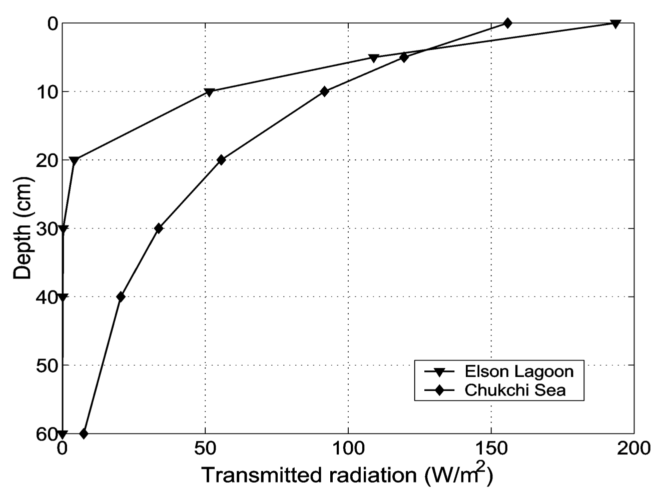

Figure 5: Transmitted radiation as predicted by a radiative transfer model in clean (CS) and sea ice on June 14 with the sediment concentration profile as depicted in Figure 4.

extent and depth of puddles are influenced by differences in topography between the EL and CS sites, a study on absorption of solar energy in contaminated sea ice has shown that high sediment concentrations result in greater pond depth (Makshtas and Podgorny, 1996, Podgorny and Grenfell, 1996). In terms of total energy used for heating the upper 20 cm of the ice by solar radiation on June 14 this amounts to 8.6 MJ/m^2 for the CS ice and 16.4 MJ/m^2 for the EL ice. This corresponds to the amount of energy required for melting 2.8 cm and 5.3 cm of ice, respectively.

CONCLUSION

The heat budget of sediment-laden and clean sea ice have been compared. It was found that sea ice with a very high sediment concentration attenuates most of the incoming solar radiation within the uppermost 20 cm, whereas clean ice transmits 35 % of the radiation at the surface to ice below 20 cm and the ocean. In conjunction with slightly delayed snow melt, this process significantly affects the temperature distribution in the sediment-laden ice of Elson Lagoon near Barrow, Alaska. While the lower layers of the ice are prevented from warming, surface ablation is increased in the dirty ice resulting in greater depth and extent of meltponds, whereas in the clean CS ice a lesser fraction of energy from solar radiation contributes to warming and melting of the top layer.

Acknowledgments
We thanks the Barrow Arctic Science Consortium (BASC), especially Dave Ramey, for logistical support. Financial support from the National Science Foundation (OPP-9872573 and OPP-9910888), is greatfully acknowledged. C. Marty kindly provided ARM radiation data.

REFERENCES

Eicken H., J. Kolatschek, J. Freitag, F. Lindemann, H. Kassens, and I. Dmitrenko (2000): Identifying a major source area and constraints on entrainment for basin-scale sediment transport by Arctic sea ice. Geophys. Res. Lett., 27, 1919-1922.

Light B., H. Eicken, G. A. Maykut, and T. C. Grenfell (1998): The effect of included particulates on the optical properties of sea ice. J. Geophys. Res., 103, 27739-27752.

Makshtas A. P., and I. A. Podgorny (1996): Calculation of melt pond albedos on Arctic sea ice. Polar Research, 15(1), 43-52.

Osterkamp T. E., and J. P. Gosink (1984): Observations and analyses of sediment-laden sea ice. In: The Alaskan Beaufort Sea: ecosystems and environments, Barnes P. W., Schell D. M., and Reimnitz E. (editors), Academic Press, Orlando, 73-93.

Perovich D. K. (1998): Optical properties of sea ice. In: Physics of ice-covered seas, vol. 1, Leppäranta M. (editor), University of Helsinki, Helsinki, 195-230.

Pfirman S., M. A. Lange, I. Wollenburg, and P. Schlosser (1990): Sea ice characteristics and the role of sediment inclusions in deep-sea deposition: Arctic - Antarctic comparisons. In: Geological history of the Polar Oceans: Arctic versus Antarctic, Bleil U., and Thiede J., editor, Kluwer Academic Publishers, Dordrecht, 187-211.

Podgorny I. A., and T. C. Grenfell (1996): Absorption of solar energy in a cryoconite hole. Geophys. Res. Lett., 23, 2465-2468.

Reimnitz E., D. Dethleff, and D. Nürnberg (1994): Contrasts in Arctic shelf sea-ice regimes and some implications: Beaufort Sea and Laptev Sea. Mar. Geol., 119, 215-225.